

CFCPalsy: Facial Image Synthesis with Cross-Fusion Cycle Diffusion Model for Facial Paralysis Individuals

Weixiang Gao Yifan Xia[†]
Shandong University

gaoweixiang@mail.sdu.edu.cn xiayifan@sdu.edu.cn

Abstract

Currently, the diagnosis of facial paralysis remains a challenging task, often relying heavily on the subjective judgment and experience of clinicians, which can introduce variability and uncertainty in the assessment process. One promising application in real-life situations is the automatic estimation of facial paralysis. However, the scarcity of facial paralysis datasets limits the development of robust machine learning models for automated diagnosis and therapeutic interventions. To this end, this study aims to synthesize a high-quality facial paralysis dataset to address this gap, enabling more accurate and efficient algorithm training. Specifically, a novel Cross-Fusion Cycle Palsy Expression Generative Model (CFCPalsy) based on the diffusion model is proposed to combine different features of facial information and enhance the visual details of facial appearance and texture in facial regions, thus creating synthetic facial images that accurately represent various degrees and types of facial paralysis. We have qualitatively and quantitatively evaluated the proposed method on the commonly used public clinical datasets of facial paralysis to demonstrate its effectiveness. Experimental results indicate that the proposed method surpasses state-of-the-art methods, generating more realistic facial images and maintaining identity consistency. [Code Link](#)

1. Introduction

Facial palsy, which can result in temporary or permanent weakness or paralysis of one side of the face, affects approximately 23 out of every 100,000 people annually [16]. Beyond the physical discomfort, patients with facial palsy often experience significant psychological distress [22]. Accurate and timely diagnosis is crucial for effective treatment; however, the variability in clinical presentation poses significant challenges, and the severity estimation of facial palsy remains a largely subjective process

[†]Corresponding author

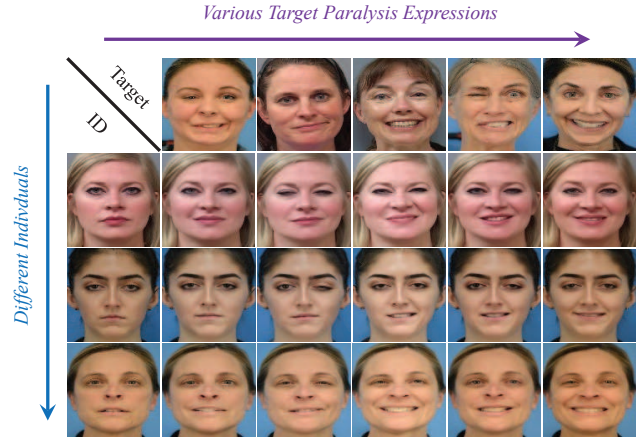


Figure 1. Facial palsy synthesis results. Each row contains images from the same individual, and each column shows images with the same facial palsy expression.

[16].

In recent years, machine learning (ML) has shown promise in aiding the diagnosis of facial paralysis by analyzing facial features and expressions [1, 15, 16, 63]. However, the development of reliable ML models is hindered by the scarcity of comprehensive, annotated datasets that accurately represent the diversity and severity of facial paralysis. Obtaining high-quality facial images of facial palsy patients is a significant challenge due to several factors, including the need to protect patient privacy and the inherent sensitivity of medical data. Additionally, the complexity of the condition and the high labor costs involved make it challenging to collect a diverse and representative dataset. Existing datasets [18, 25, 65] are often limited in size, scope, and variability, restricting the generalization ability and performance of ML algorithms.

Several studies have explored the use of generative adversarial networks (GANs) [17] to generate facial paralysis face images [50, 51, 67]. Although [67] successfully utilizes GANs to simulate facial expressions by reconstructing facial images from extracted boundary information, the

generated images often lack the fine details necessary for accurate medical diagnosis, especially when there is a significant disparity between the facial features of the patient and the face to be combined with the palsy features. Building on this, another study [51] introduces facial shape normalization to address the unnatural appearance of images resulting from shape differences between the patient and the model. While this method improves image realism, it still struggles with capturing complex facial expressions and fine details, limiting its effectiveness in more nuanced diagnostic scenarios. In addition, to leverage data augmentation, GANs are also used to improve the performance of convolutional neural networks (CNNs) in grading facial palsy [50]. This approach synthesizes additional face images with varying degrees of facial palsy to combat overfitting and enhance the model’s generalization capability. However, the synthesized images in this study primarily focus on only five categories without adequately capturing the full range of facial expressions and subtle asymmetries inherent in real-world cases.

In this paper, we aim to address the critical need for a comprehensive facial paralysis dataset by synthesizing a high-quality dataset. The generator is designed to capture a wide range of facial paralysis conditions and able to generate face images with varying degrees of facial paralysis based on a given facial identity image, providing a valuable resource for training ML models with the potential to improve diagnostic accuracy and clinical outcomes.

To this end, we propose a Cross-Fusion Cycle Palsy Expression Generative Model (CFCPalsy). CFCPalsy is a unique triple condition image generation model, conditioned on identity information of a given ID image, expression information and landmark information of a given style image. It could generate a realistic image of the face in the ID image exhibiting the facial palsy characteristics of the face in the style image. CFCPalsy employs landmark features and the corresponding loss to ensure that the model could fully capture the nuanced facial deformations, particularly the detailed changes in facial features such as eyes, mouth, and overall asymmetry. When the model is fed multiple features simultaneously, it often encounters challenges such as feature redundancy and conflicting information, which can lead to degraded performance [36]. The redundancy among features can cause the model to overweight certain aspects, while conflicting signals may lead to inconsistent learning and prediction. To address these issues, CFCPalsy utilizes a novel cross-fusion feature integration method. This approach effectively harmonizes the information from multiple features, enabling the model to better leverage the complementary aspects of each feature, thereby significantly improving the overall performance and robustness of the model. Training diffusion models [20, 54] on limited datasets often leads to inefficiencies in learning

and suboptimal model performance due to the scarcity of data. To address these challenges, we focused on improving the training efficiency and overall performance of diffusion models under constrained data conditions by modifying the training strategy. Our approach optimizes the learning process and proposes the cycle diffusion framework enabling the model to achieve superior results with a limited dataset.

On the whole, the contributions of this paper are summarized as follows:

- We first combine diffusion models with landmark features to improve the quality of facial synthesis and introduce a clever feature confusion strategy that substantially improves the model’s capability to effectively learn from various features.
- We propose a cycle framework for diffusion models, which provides an innovative approach to train higher-performance models with limited datasets.
- Our approach introduces a novel application of generative models for facial paralysis synthesis, achieving state-of-the-art results and addressing the scarcity of medical datasets, thereby facilitating future research in automated facial analysis.

2. Related Work

Face Synthesis Face generation has become a prominent area of research within computer vision, driven by advancements in generative models such as Generative Adversarial Networks (GANs) [17], Variational Autoencoders (VAEs) [32, 35, 48, 55], and diffusion models [20, 54]. Among these, GANs have been extensively utilized for various tasks such as face generation and augmentation [9, 23, 37, 45, 59, 66]. Various methods have been developed to ensure that the generated face retains the original identity while allowing for other modifications such as image styles or background [2, 5, 6, 11, 47, 53, 60, 68]. To attain a better performance, researchers have recently turned to diffusion models [24, 58, 69], which offer a more stable and probabilistic framework for face image generation. DCFace [31] proposes a dual-condition diffusion model that generates synthetic face datasets, producing high-quality face images with varied identities and styles. Our work investigates how the severity of facial palsy and changes in facial expressions influence the synthesis of realistic images.

Diffusion Models Diffusion models [20, 54] have emerged as a robust alternative to GANs for a wide range of image generation tasks [12]. Unlike GANs, which rely on an adversarial framework, diffusion models gradually refine noisy inputs through a series of steps, leading to more stable and high-fidelity outputs. Several studies [21, 27, 39, 52, 56] have employed advanced sampling strategies that enhance both the efficiency and the output quality of diffusion models such as the latent space diffu-

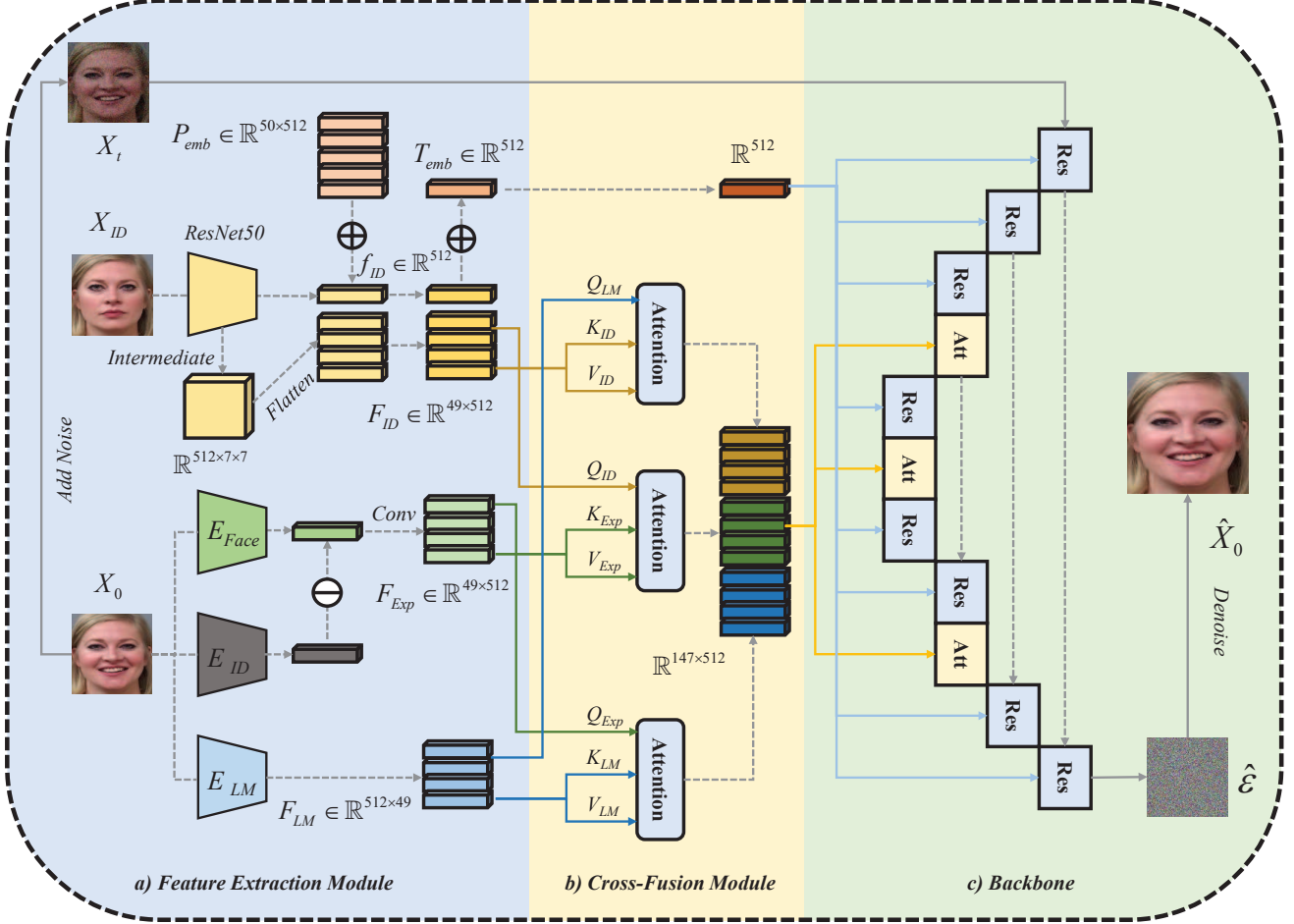


Figure 2. An overview of the forward process of CFCPalsy. a) The architecture of our feature extractors. We train the model using different images of the same patient, with one serving as the identity image X_{ID} and the other as the facial palsy expression image X_0 . The identity model extracts identity features from the identity image. The expression module (including E_{Face} and E_{ID}) and E_{LM} extract expression and landmark features from the facial palsy expression image, respectively. b) An illustration of the principle of the cross feature fusion strategy. We employ a method similar to cross-attention to facilitate information exchange among the three conditional features. After this interaction, the features are concatenated for further processing. c) A diagram of the noise predicting network. CFCPalsy utilizes a classic U-Net architecture combined with residual connections and cross-attention mechanisms to accurately predict the noise.

sion [14, 41, 44, 49, 61]. In addition, there are also studies [4, 13, 27–30, 33, 43, 57, 72] focused on enhancing the models’ training efficiency by modifying the training strategies. We propose a novel cycle diffusion strategy that integrates the second loss setting designed to enhance model performance, particularly when training on limited datasets.

3. Method

In this section, we present our Cross-Fusion Cycle Palsy Expression Model (CFCPalsy) designed to synthesize high-quality facial paralysis images (see Fig. 2). First, we mention the necessary preliminary concepts about the diffusion models (sec 3.1). Next, we introduce the various feature extractors used in CFCPalsy which enhance the diffusion

model’s ability to capture more facial details by accurately extracting multiple features (sec 3.2). In sec 3.3, we propose the cross feature fusion, which mitigates the model’s over-reliance on individual features and enhances its overall learning capability across all features by exchanging query vectors formed from different features. Finally, we devise the cycle training strategy that improves the training efficiency and performance of the diffusion model on limited datasets by modifying the training process and introducing a secondary loss function (sec 3.4).

3.1. Preliminary

Diffusion models [20, 54] are a class of generative models that define a forward process, where data is gradually corrupted by noise, and a reverse process, which learns

to denoise and recover the original data distribution. The forward process is typically modeled by a discrete-time Markov chain [40], where at each time step t , the data X_t is obtained by adding Gaussian noise to the data from the previous step X_{t-1} , following the equation:

$$q(X_t | X_{t-1}) = \mathcal{N}(X_t; \sqrt{1 - \beta_t} X_{t-1}, \beta_t I), \quad (1)$$

where β_t is a variance schedule that controls the amount of noise added at each step. The reverse process aims to estimate the posterior distribution $p_\theta(X_{t-1} | X_t)$, which is modeled by a neural network parameterized by θ . The training objective is to minimize the variational bound on the negative log-likelihood, which often reduces to a simplified mean squared error loss between the true noise and the noise predicted by the model:

$$L(\theta) = \mathbb{E}_{t, X_t, \epsilon} [\|\epsilon - \epsilon_\theta(X_t, t)\|^2], \quad (2)$$

where ϵ is the true noise and $\epsilon_\theta(X_t, t)$ is the model's prediction. By iteratively applying this reverse process, the model is able to generate new data samples from pure noise, refining them step by step until the desired output is obtained. Building on this foundation, we employ a two-stage diffusion process along with a more complex loss function to enhance training efficiency and improve the quality of the generated outputs.

3.2. Feature Extraction Module

ID Extraction Module To accurately capture identity information from X_{ID} , we use the IR-50 [10], a typical CNN, as the identity feature extractor. We utilize both the output features $f_{ID} \in \mathbb{R}^{512}$ from the final layer and the intermediate layer features $I_{ID} \in \mathbb{R}^{512 \times 7 \times 7}$ of the model to enhance the quality of image generation. For I_{ID} , we first flatten and rearrange their dimensions to obtain $F_{ID} \in \mathbb{R}^{49 \times 512}$ that facilitates subsequent processing. Then, we concatenate the two sets of features and add positional embeddings P_{emb} . In summary, the output of the identity feature extraction module M_{ID} is formulated as follows:

$$M_{ID}(X_{ID}) = \text{Concat}[f_{ID}, \text{Flatten}(I_{ID})] + P_{emb}. \quad (3)$$

For the output features, we process the intermediate feature part and the final layer feature part separately by injecting them into different model blocks, rather than concatenating them together. The identity feature extractor is trainable during the diffusion model training process to effectively extract identity features.

Expression Extraction Module CFPPalsy employs the deviation framework of DLN [71] to accurately capture the expression features. This module M_{Exp} consists of two models: a facial feature extraction model E_{Face} and an identity feature extraction model E_{ID} , sharing the same

network structure. Based on the assumption that facial features can be divided into identity features and expression features, we use two separate models to extract expression and identity features from the same facial paralysis image X_0 . By subtracting the identity features from the facial features, we obtain expression features that are invariant to identity. The subtracted features are then passed through a convolution operation for channel alignment. Specifically,

$$M_{Exp}(X_0) = \text{Conv}[E_{Face}(X_0) - E_{ID}(X_0)]. \quad (4)$$

Landmark Extractor Facial landmarks refer to key points on a face such as the corners of the eyes, the tip of the nose, and the edges of the lips that are used to represent and understand facial geometry, which could enhance facial generation by imposing constraints on critical facial regions. For the first time, we integrate facial landmark features with diffusion models, coupled with a specifically designed loss function, to generate realistic and detailed facial images of patients with facial palsy. In our CFPPalsy, we employ the MobileFaceNet [7] as the landmark detector. We remove its output layer to use it as a landmark feature extractor E_{LM} , which outputs a feature $F_{LM} \in \mathbb{R}^{49 \times 512}$.

3.3. Cross-Fusion Module

The attention mechanism [62] has become a fundamental component in many state-of-the-art models, particularly for tasks requiring the integration of information from different sources or across different parts of a data sequence. At its core, the attention mechanism allows a model to weigh the importance of different elements within a sequence, dynamically focusing on the most relevant parts to improve decision-making or feature extraction. The cross-attention mechanism extends this concept to operate between two distinct sequences. This facilitates the fusion of information from different sources, making it particularly useful for tasks that require integrating features from multiple modalities or input streams.

We aim for the model to fully utilize the information from identity, expression, and landmarks when predicting noise. Although directly concatenating the features from these three sources and injecting them into the model is a feasible approach, it does not yield satisfactory results. The generated images either lose the identity information from identity images X_{ID} or fail to retain the facial expression details from original images X_0 . Building on the concept of the cross-attention mechanism, we perform mutual interaction among multiple features, where the query sequence from one feature guides the extraction of information from the key-value sequence of another feature.

The features from the extractors are first mapped into the query, key, and value vector spaces separately through a QKV encoder. Specifically,

$$Q = FW^Q, K = FW^K, V = FW^V, \quad (5)$$

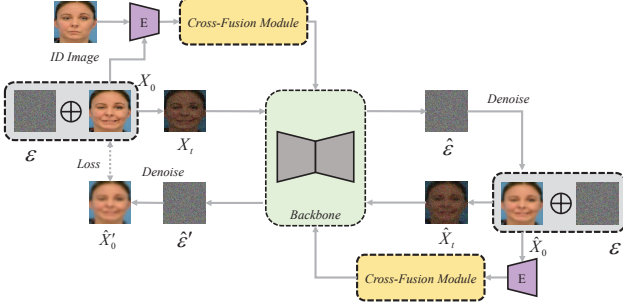


Figure 3. An illustration of the cycle training strategy of CFC-Palsy. Each training data undergoes two diffusion processes, where the plus sign indicates the noise addition process.

where F indicates the three types of features extracted from the former modules, and W^Q, W^K, W^V represent the model’s learnable parameter matrixes. Similar to the multi-head attention mechanism [62], we utilize multiple sets of transformation matrices to obtain multiple vector spaces, aiming to capture different interaction patterns among features.

Subsequently, the identity features, expression features, and landmark features each have their own corresponding QKV vector spaces. Next, we perform vector interactions. Specifically,

$$\text{Attention}_{ID} = \text{Softmax} \left(\frac{Q_{LM} K_{ID}^T}{\sqrt{d_k}} \right) V_{ID}, \quad (6)$$

$$\text{Attention}_{Exp} = \text{Softmax} \left(\frac{Q_{ID} K_{Exp}^T}{\sqrt{d_k}} \right) V_{Exp}, \quad (7)$$

$$\text{Attention}_{LM} = \text{Softmax} \left(\frac{Q_{Exp} K_{LM}^T}{\sqrt{d_k}} \right) V_{LM}, \quad (8)$$

where d_k is a scaling factor.

3.4. Cycle Diffusion Strategy

Building upon the training framework of the original diffusion model, we incorporated an additional step of secondary diffusion. Algorithm 1 shows the training procedure of CFC-Palsy. After the original diffusion process, where the input image X_0 is noised to generate a noisy image X_t , and the network predicts the noise ϵ_θ to restore the original image \hat{X}_0 . Based on the equation

$$\hat{X}_0 = \frac{1}{\sqrt{\alpha_t}} (X_t - \sqrt{1 - \alpha_t} \epsilon_\theta(X_t, t)), \quad (9)$$

where $\bar{\alpha}_t$ is a term that accumulates the effects of the noise schedule over time, often defined as the product $\bar{\alpha}_t = \prod_{s=1}^t \alpha_s$, with α_s being a scalar controlling the amount of noise added at each time step, we further introduced a

secondary diffusion step (see Fig. 3). In this step, the predicted image \hat{X}_0 is treated as the new input image, which is subjected to the same noise addition process to obtain a secondary noisy image \hat{X}_t . This secondary noisy image is then fed into the noise prediction network to generate a secondary predicted noise ϵ'_θ , which is subsequently used to restore the once-noised image.

For the first diffusion process, we utilized a weighted combination of mean square error loss (see Eq. 2), identity consistency loss L_{ID} (the same as the Time-step Dependent ID Loss in DCFace [31]), and landmark loss L_{LM} as our first loss function. The identity consistency loss L_{ID} is derived from the cosine similarity between the identity features extracted from the images, while the landmark loss L_{LM} is obtained by calculating the mean squared error of the detected landmark keypoints:

$$L_{first} = L(\theta) + \lambda L_{ID}(X_{ID}, \hat{X}_0) + \gamma L_{LM}(X_0, \hat{X}_0), \quad (10)$$

To align with the architecture of CFC-Palsy, we introduced the concept of a secondary loss function to enhance the effectiveness of the model’s training, whose basic composition is consistent with that of the first loss. However, the noisy image \hat{X}_t generated from \hat{X}_0 does not participate in the denoising process after the second diffusion, and \hat{X}_0 itself is also excluded from the calculation of the second loss. Instead, we calculate the respective loss components using the original image X_0 before the first diffusion and the restored predicted image \hat{X}_0' after the second denoising. Specifically,

$$L_{second} = L(\theta') + \lambda L_{ID}(X_{ID}, \hat{X}_0') + \gamma L_{LM}(X_0, \hat{X}_0'), \quad (11)$$

The final loss is the weighted sum of the first loss and the second loss.

Algorithm 1 Training Algorithm of CFC-Palsy

```

for every batch do
  for  $(x_0, x_{id})$  in the batch do
    Sample  $\epsilon \sim \mathcal{N}(0, I)$ 
    Sample  $t \sim \text{Uniform}(\{0, 1, 2, \dots, T\})$ 
    Perform initial diffusion
     $x_t = \sqrt{\alpha_t} x_0 + \sqrt{1 - \alpha_t} \epsilon$ 
     $\hat{x}_0 = \frac{1}{\sqrt{\alpha_t}} (x_t - \sqrt{1 - \alpha_t} \epsilon_\theta(x_t, x_{id}, t))$ 
    Calculate  $\mathcal{L}_{first}$ 
    Perform second diffusion
     $x'_t = \sqrt{\alpha_t} \hat{x}_0 + \sqrt{1 - \alpha_t} \epsilon$ 
     $\hat{x}'_0 = \frac{1}{\sqrt{\alpha_t}} (x'_t - \sqrt{1 - \alpha_t} \epsilon'_\theta(x'_t, x_{id}, t))$ 
    Calculate  $\mathcal{L}_{second}$ 
    Update with  $\mathcal{L} = \mathcal{L}_{first} + \sigma \mathcal{L}_{second}$ 
  end for
end for

```

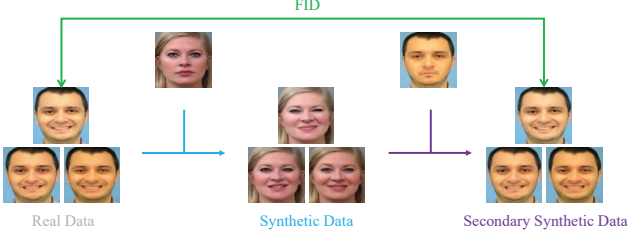


Figure 4. A schematic diagram of the aFID calculation method. Calculate the FID value between the twice-synthesized data and the original data.

4. Experiments

4.1. Datasets

AFLFP: The Annotated Facial Landmarks for Facial Palsy (AFLFP) [65] dataset is a comprehensive and laboratory-controlled collection designed to support the analysis of facial paralysis. It consists of facial images from 88 subjects, each participating in 16 different expression videos, such as brow raise, closed smile, gentle eye closure, and open smile. For each expression, the dataset captures keyframes representing four critical states: neutral, onset, a mid-state between onset and peak, and peak. In total, the AFLFP dataset contains 5,632 facial images, with 1,408 images corresponding to each key state and 64 images per subject.

MEEI: The Massachusetts Eye and Ear Infirmary (MEEI) [18] dataset is a carefully curated collection focused on facial palsy, comprising both videos and high-resolution images. The dataset includes 60 videos from a diverse group of participants, consisting of 9 healthy subjects and 51 patients with varying degrees of facial paralysis. Each video captures 8 distinct facial movements, which are also provided as individual images, resulting in a total of 480 high-resolution images. The subjects in the MEEI dataset are categorized based on their eFACE [3] scores, which assess the severity of facial palsy.

4.2. Evaluation Metrics

To evaluate the effectiveness of image generation from different perspectives, for the synthesized images, we compute Peak Signal-to-Noise Ratio (PSNR), Structural Similarity Index Measure (SSIM) [64], Learned Perceptual Image Patch Similarity (LPIPS) [70], Perceptual Loss (PL) [26], on unseen data. For this multi-condition synthesis task, we compute these metrics separately for identity images and facial paralysis expression images to simultaneously evaluate identity preservation and expression transfer.

Fréchet Inception Distance (FID) [19] is widely used to evaluate the quality of image generation. It measures the distance between the distribution of generated images and real images by comparing the statistics of feature repre-

sentations extracted from a pre-trained Inception network. A lower FID score indicates that the generated images are more similar to the real images, both in terms of visual quality and diversity. However, some studies [8, 46] have shown that inconsistencies in the class distribution between the generated dataset and the real dataset can affect the calculation of the FID score.

To address this issue, we propose the aligned FID (aFID) (See Fig. 4) to evaluate the quality of the multi-condition diffusion model. Specifically, for each facial palsy patient in the test set, we first use images of other individuals as identity images and the patient’s condition image as the facial palsy expression image. This process synthesizes an image where the patient’s facial palsy expression is transferred onto another individual. We then use this generated dataset as the facial palsy expression images and the original facial palsy patient’s images as identity images to generate a second set of synthetic images. Finally, we calculate the FID score between this generated dataset and the real dataset. Ideally, the images in these two datasets should be identical.

4.3. Implementation details

For the identity feature extractor E_{ID} , we utilized the same IR-50 [10] as DCFace [31]. Intermediate features from this network were injected into the cross-fusion module, and the final features were incorporated into the model prediction network with timesteps, and after initialization from DCFace, the model is trained end-to-end. For both the identity model and the face model within the expression extracting module, we also used the IR-50 architecture. After the same initialization, the ID model’s weights were fixed, and the module was trained on the AffectNet [42] dataset, after which the module’s weights were all fixed. For the landmark extractor E_{LM} and detector D_{LM} , we used the MobileFaceNet [7] and fixed its weights to obtain the landmark information. For each patient’s video in the MEEI dataset, we performed frame extraction. Keyframes representing eight different expressions for each facial palsy patient were manually selected. Each expression consists of 32 frames, capturing the full expression process from onset, development, peak, dissipation, to a neutral state. For the images in AFLFP and MEEI, we first performed face extraction and segmented them into 112x112 facial images. After removing low-quality images and those with poor segmentation quality, we ultimately obtained 91,168 facial images from 313 individuals. We used 88% of the data (80,288 images from 276 individuals) for the model’s training set, while 12% of the data (10,880 images from 37 individuals) was set aside as the test set for subsequent evaluation metric calculations. CFCPalsy was trained on the training set using the AdamW Optimizer [34, 38] for 10 epochs with a learning rate of 0.0001, utilizing two NVIDIA RTX 4090



Figure 5. Visualized experimental results. CFCPalsy is the standard version, CFCPalsy¹ is the CFCPalsy without facial landmarks, CFCPalsy² excludes the cycle training strategy and CFCPalsy³ operates in the absence of the cross-fusion module.

GPUs.

4.4. Ablation Study

To evaluate the contribution of each component in our model, we conducted a series of ablation studies. These experiments assess the impact of removing or altering key modules on the model’s performance. The visualization results of the ablation study are shown in Fig 5. The quantitative

results are shown in Tab. 1.

Facial Landmarks To investigate the role of facial landmark features in image generation, we remove the facial landmark condition from CFCPalsy. The model no longer learns landmark features, and in the fusion module, only identity features and expression features are used for information exchange through query key interactions and concatenation. During training, the model also stops using the

Table 1. Quantitative results on the test set.

Method					Metrics								
Model	GS	LM	CF	CD	aFID ↓	PSNR ↑		SSIM ↑		LPIPS ↓		PL ↓	
						X _{ID}	X _{Style}	X _{ID}	X _{Style}	X _{ID}	X _{Style}	X _{ID}	X _{Style}
DCFace [31]	3x3	-	-	-	56.77	15.95	17.07	0.32	0.35	0.37	0.34	0.27	0.24
	5x5	-	-	-	56.20	17.15	19.39	0.40	0.48	0.34	0.26	0.26	0.19
CFCPalsy	-	×	✓	✓	50.47	17.31	16.05	0.45	0.40	0.31	0.33	0.25	0.28
	-	✓	×	✓	54.42	17.13	15.99	0.47	0.44	0.31	0.33	0.26	0.26
	-	✓	✓	×	45.69	17.41	16.31	0.47	0.43	0.32	0.34	0.25	0.28
	-	✓	✓	✓	43.76	17.44	16.36	0.47	0.45	0.31	0.33	0.25	0.27

GS = Grid Size, LM = Facial Landmark Features, CF = Cross-Fusion Module, CD = Cycle Diffusion Strategy.

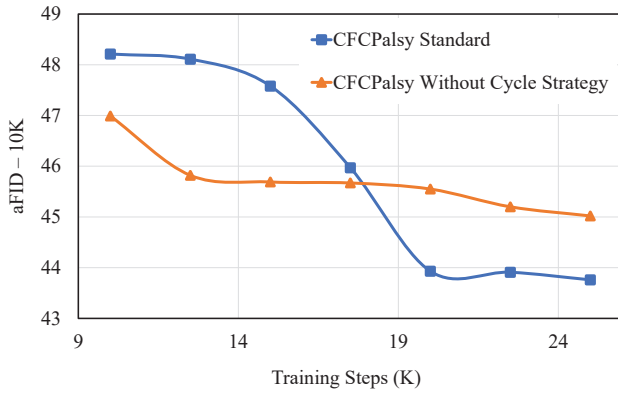


Figure 6. Ablation results for the Cycle Diffusion Training Strategy, tracking training steps to calculate aFID on the test set.

landmark loss for weight updates. The results in Tab. 1 show a significant increase in aFID, and the pixel-level comparison metrics for facial palsy expression also exhibit a clear decline. As seen in Fig. 5, the model is largely unable to correctly learn facial palsy expressions. This highlights the importance of facial landmark features in synthesizing detailed facial palsy expressions.

Cross-Fusion Module Tab. 1 compares the performance of the model with and without the cross-fusion module. It can be observed that directly concatenating multiple features and injecting them into the model leads to a sharp increase in aFID by 10.66, making it the component with the most significant impact on overall performance. Combined with other metrics, this shows that the cross-fusion module plays a crucial role in improving both identity preservation and facial palsy feature transfer. This feature fusion module effectively enhances the model’s ability to learn from multiple features comprehensively.

Cycle Training Strategy The design of Cycle Diffusion is intended to improve the training efficiency of the model on limited datasets. We conducted comparative experiments to verify the effectiveness of this strategy. As shown in Tab.

1, the cycle training strategy provides a noticeable performance improvement for the model. We tracked the training process and plotted the changes in aFID, with the results shown in Fig. 6. Compared to the standard diffusion model training strategy, Cycle Diffusion achieves higher training efficiency.

4.5. Comparison with Previous Methods

We compared CFCPalsy with a similar facial synthesis task, DCFace [31], using 3x3 and 5x5 grid sizes on unseen images. The visual comparison results and numerical comparison results are shown in Fig. 5 and Tab. 1, respectively. Although DCFace 5x5 achieves better scores in several generated data and facial palsy expression data metrics, this does not necessarily indicate a higher degree of facial palsy feature transfer. Pixel-level and perception-based metrics not only focus on facial expressions but also consider factors like lighting and background, which are not primary considerations in the task of facial palsy synthesis. Compared to DCFace 5x5, aFID of images generated by CFCPalsy decreases by approximately 22%, and CFCPalsy also demonstrates a clear advantage in terms of identity feature preservation.

5. Conclusion

Our research proposes Cross-Fusion Cycle Palsy Expression Generative Model (CFCPalsy), based on the conditional diffusion model, utilizing multiple feature extractors to accurately capture various facial features, employing a cross-fusion module to integrate these features and applying a cycle training strategy to improve training efficiency and effectiveness. As a result, CFCPalsy generates realistic facial palsy expression images, providing valuable training data for machine learning systems used in facial palsy diagnosis and treatment assistance. Results indicate that CFCPalsy surpasses existing methods in several metrics, including aFID, PSNR, and SSIM, achieving excellent performance.

References

- [1] Ali Saber Amsalam, Ali Al-Naji, and Ammar Yahya Daeeif. Facial palsy detection using pre-trained deep learning models: A comparative study. In *AIP Conference Proceedings*. AIP Publishing, 2024. 1
- [2] Gwangbin Bae, Martin de La Gorce, Tadas Baltrušaitis, Charlie Hewitt, Dong Chen, Julien Valentin, Roberto Cipolla, and Jingjing Shen. Digiface-1m: 1 million digital face images for face recognition. In *Proceedings of the IEEE/CVF Winter Conference on Applications of Computer Vision*, 2023. 2
- [3] Caroline A Banks, Prabhat K Bhamra, Jong Park, Charles R Hadlock, and Tessa A Hadlock. Clinician-graded electronic facial paralysis assessment: the eface. *Plastic and reconstructive surgery*, 2015. 6
- [4] Fan Bao, Chongxuan Li, Jiacheng Sun, Jun Zhu, and Bo Zhang. Estimating the optimal covariance with imperfect mean in diffusion probabilistic models. *arXiv preprint arXiv:2206.07309*, 2022. 3
- [5] Jianmin Bao, Dong Chen, Fang Wen, Houqiang Li, and Gang Hua. Cvae-gan: fine-grained image generation through asymmetric training. In *Proceedings of the IEEE international conference on computer vision*, 2017. 2
- [6] Jianmin Bao, Dong Chen, Fang Wen, Houqiang Li, and Gang Hua. Towards open-set identity preserving face synthesis. In *Proceedings of the IEEE conference on computer vision and pattern recognition*, 2018. 2
- [7] Cunjian Chen. Pytorch face landmark: A fast and accurate facial landmark detector, 2021. 4, 6
- [8] Yang Chen, Dustin J Kempton, and Rafal A Angryk. Examining effects of class imbalance on conditional gan training. In *International Conference on Artificial Intelligence and Soft Computing*. Springer, 2023. 6
- [9] Yunje Choi, Minje Choi, Munyoung Kim, Jung-Woo Ha, Sunghun Kim, and Jaegul Choo. Stargan: Unified generative adversarial networks for multi-domain image-to-image translation. In *Proceedings of the IEEE conference on computer vision and pattern recognition*, 2018. 2
- [10] Jiankang Deng, Jia Guo, Niannan Xue, and Stefanos Zafeiriou. Arcface: Additive angular margin loss for deep face recognition. In *Proceedings of the IEEE/CVF conference on computer vision and pattern recognition*, 2019. 4, 6
- [11] Yu Deng, Jiaolong Yang, Dong Chen, Fang Wen, and Xin Tong. Disentangled and controllable face image generation via 3d imitative-contrastive learning. In *Proceedings of the IEEE/CVF conference on computer vision and pattern recognition*, 2020. 2
- [12] Prafulla Dhariwal and Alexander Nichol. Diffusion models beat gans on image synthesis. *Advances in neural information processing systems*, 2021. 2
- [13] Tim Dockhorn, Arash Vahdat, and Karsten Kreis. Score-based generative modeling with critically-damped langevin diffusion. *arXiv preprint arXiv:2112.07068*, 2021. 3
- [14] Alex Ergasti, Claudio Ferrari, Tomaso Fontanini, Massimo Bertozzi, and Andrea Prati. Towards controllable face generation with semantic latent diffusion models. *arXiv preprint arXiv:2403.12743*, 2024. 3
- [15] Amira Gaber, Mona F Taher, Manal Abdel Wahed, Nevin Mohieldin Shalaby, and Sarah Gaber. Classification of facial paralysis based on machine learning techniques. *BioMedical Engineering OnLine*, 2022. 1
- [16] Xuri Ge, Joemon M Jose, Pengcheng Wang, Arunachalam Iyer, Xiao Liu, and Hu Han. Automatic facial paralysis estimation with facial action units. *arXiv preprint arXiv:2203.01800*, 2022. 1
- [17] Ian Goodfellow, Jean Pouget-Abadie, Mehdi Mirza, Bing Xu, David Warde-Farley, Sherjil Ozair, Aaron Courville, and Yoshua Bengio. Generative adversarial nets. *Advances in neural information processing systems*, 2014. 1, 2
- [18] Jacqueline J Greene, Diego L Guarin, Joana Tavares, Emily Fortier, Mara Robinson, Joseph Dusseldorp, Olivia Quatela, Nate Jowett, and Tessa Hadlock. The spectrum of facial palsy: The meei facial palsy photo and video standard set. *The Laryngoscope*, 2020. 1, 6
- [19] Martin Heusel, Hubert Ramsauer, Thomas Unterthiner, Bernhard Nessler, and Sepp Hochreiter. Gans trained by a two time-scale update rule converge to a local nash equilibrium. *Advances in neural information processing systems*, 2017. 6
- [20] Jonathan Ho, Ajay Jain, and Pieter Abbeel. Denoising diffusion probabilistic models. *Advances in neural information processing systems*, 2020. 2, 3
- [21] Jonathan Ho and Tim Salimans. Classifier-free diffusion guidance. *arXiv preprint arXiv:2207.12598*, 2022. 2
- [22] Matthew Hottot, Esme Huggons, Claire Hamlet, Danielle Shore, David Johnson, Jonathan H Norris, Sarah Kilcoyne, and Louise Dalton. The psychosocial impact of facial palsy: a systematic review. *British Journal of Health Psychology*, 2020. 1
- [23] Qiyang Hu, Attila Szabó, Tiziano Portenier, Paolo Favaro, and Matthias Zwicker. Disentangling factors of variation by mixing them. In *Proceedings of the IEEE Conference on Computer Vision and Pattern Recognition*, 2018. 2
- [24] Ziqi Huang, Kelvin CK Chan, Yuming Jiang, and Ziwei Liu. Collaborative diffusion for multi-modal face generation and editing. In *Proceedings of the IEEE/CVF Conference on Computer Vision and Pattern Recognition*, 2023. 2
- [25] Gee-Sern Jison Hsu, Wen-Fong Huang, and Jiunn-Horng Kang. Hierarchical network for facial palsy detection. In *Proceedings of the IEEE Conference on Computer Vision and Pattern Recognition Workshops*, 2018. 1
- [26] Justin Johnson, Alexandre Alahi, and Li Fei-Fei. Perceptual losses for real-time style transfer and super-resolution. In *European Conference on Computer Vision (ECCV)*, 2016. 6
- [27] Tero Karras, Miika Aittala, Timo Aila, and Samuli Laine. Elucidating the design space of diffusion-based generative models. *Advances in neural information processing systems*, 2022. 2, 3
- [28] Tero Karras, Miika Aittala, Jaakko Lehtinen, Janne Hellsten, Timo Aila, and Samuli Laine. Analyzing and improving the training dynamics of diffusion models. In *Proceedings of the IEEE/CVF Conference on Computer Vision and Pattern Recognition*, 2024.
- [29] Daegyu Kim, Jooyoung Choi, Chaehun Shin, Uiwon Hwang, and Sungroh Yoon. Improving diffusion-based generative models via approximated optimal transport. *arXiv preprint arXiv:2403.05069*, 2024.

- [30] Dongjun Kim, Seungjae Shin, Kyungwoo Song, Wanmo Kang, and Il-Chul Moon. Soft truncation: A universal training technique of score-based diffusion model for high precision score estimation. *arXiv preprint arXiv:2106.05527*, 2021. 3
- [31] Minchul Kim, Feng Liu, Anil Jain, and Xiaoming Liu. Dc-face: Synthetic face generation with dual condition diffusion model. In *Proceedings of the IEEE/CVF conference on computer vision and pattern recognition*, 2023. 2, 5, 6, 8
- [32] DP Kingma. Auto-encoding variational bayes. *arXiv preprint arXiv:1312.6114*, 2013. 2
- [33] Diederik Kingma, Tim Salimans, Ben Poole, and Jonathan Ho. Variational diffusion models. *Advances in neural information processing systems*, 2021. 3
- [34] Diederik P Kingma. Adam: A method for stochastic optimization. *arXiv preprint arXiv:1412.6980*, 2014. 6
- [35] Anders Boesen Lindbo Larsen, Søren Kaae Sønderby, Hugo Larochelle, and Ole Winther. Autoencoding beyond pixels using a learned similarity metric. In *International conference on machine learning*. PMLR, 2016. 2
- [36] Jundong Li, Kewei Cheng, Suhang Wang, Fred Morstatter, Robert P Trevino, Jiliang Tang, and Huan Liu. Feature selection: A data perspective. *ACM computing surveys (CSUR)*, 2017. 2
- [37] Jianxin Lin, Yingce Xia, Tao Qin, Zhibo Chen, and Tie-Yan Liu. Conditional image-to-image translation. In *Proceedings of the IEEE conference on computer vision and pattern recognition*, 2018. 2
- [38] I Loshchilov. Decoupled weight decay regularization. *arXiv preprint arXiv:1711.05101*, 2017. 6
- [39] Cheng Lu, Yuhao Zhou, Fan Bao, Jianfei Chen, Chongxuan Li, and Jun Zhu. Dpm-solver: A fast ode solver for diffusion probabilistic model sampling in around 10 steps. *Advances in Neural Information Processing Systems*, 2022. 2
- [40] Andrey Markov. Extension of the limit theorems of probability theory to a sum of variables connected in a chain. *Dynam Probabilist Syst*, 1971. 4
- [41] Thomas W Mitchel, Carlos Esteves, and Ameesh Makadia. Single mesh diffusion models with field latents for texture generation. In *Proceedings of the IEEE/CVF Conference on Computer Vision and Pattern Recognition*, 2024. 3
- [42] Ali Mollahosseini, Behzad Hasani, and Mohammad H Mahoor. Affectnet: A database for facial expression, valence, and arousal computing in the wild. *IEEE Transactions on Affective Computing*, 2017. 6
- [43] Alexander Quinn Nichol and Prafulla Dhariwal. Improved denoising diffusion probabilistic models. In *International conference on machine learning*. PMLR, 2021. 3
- [44] Dustin Podell, Zion English, Kyle Lacey, Andreas Blattmann, Tim Dockhorn, Jonas Müller, Joe Penna, and Robin Rombach. Sdxl: Improving latent diffusion models for high-resolution image synthesis. *arXiv preprint arXiv:2307.01952*, 2023. 3
- [45] Albert Pumarola, Antonio Agudo, Aleix M Martinez, Alberto Sanfeliu, and Francesc Moreno-Noguer. Ganimation: Anatomically-aware facial animation from a single image. In *Proceedings of the European conference on computer vision (ECCV)*, 2018. 2
- [46] Yiming Qin, Huangjie Zheng, Jiangchao Yao, Mingyuan Zhou, and Ya Zhang. Class-balancing diffusion models. In *Proceedings of the IEEE/CVF Conference on Computer Vision and Pattern Recognition*, 2023. 6
- [47] Haibo Qiu, Baosheng Yu, Dihong Gong, Zhifeng Li, Wei Liu, and Dacheng Tao. Synface: Face recognition with synthetic data. In *Proceedings of the IEEE/CVF International Conference on Computer Vision*, 2021. 2
- [48] Danilo Jimenez Rezende, Shakir Mohamed, and Daan Wierstra. Stochastic backpropagation and approximate inference in deep generative models. In *International conference on machine learning*. PMLR, 2014. 2
- [49] Robin Rombach, Andreas Blattmann, Dominik Lorenz, Patrick Esser, and Björn Ommer. High-resolution image synthesis with latent diffusion models. In *Proceedings of the IEEE/CVF conference on computer vision and pattern recognition*, 2022. 3
- [50] Muhammad Sajid, Tamoor Shafique, Mirza Jabbar Aziz Baig, Imran Riaz, Shahid Amin, and Sohaib Manzoor. Automatic grading of palsy using asymmetrical facial features: a study complemented by new solutions. *Symmetry*, 2018. 1, 2
- [51] Takato Sakai, Masataka Seo, Naoki Matsushiro, and Yen-Wei Chen. Simulation of facial palsy using conditional generative adversarial networks and face shape normalization. In *2021 IEEE 10th Global Conference on Consumer Electronics (GCCE)*. IEEE, 2021. 1, 2
- [52] Tim Salimans and Jonathan Ho. Progressive distillation for fast sampling of diffusion models. *arXiv preprint arXiv:2202.00512*, 2022. 2
- [53] Yujun Shen, Ping Luo, Junjie Yan, Xiaogang Wang, and Xiaoou Tang. Faceid-gan: Learning a symmetry three-player gan for identity-preserving face synthesis. In *Proceedings of the IEEE conference on computer vision and pattern recognition*, 2018. 2
- [54] Jascha Sohl-Dickstein, Eric Weiss, Niru Maheswaranathan, and Surya Ganguli. Deep unsupervised learning using nonequilibrium thermodynamics. In *International conference on machine learning*. PMLR, 2015. 2, 3
- [55] Casper Kaae Sønderby, Tapani Raiko, Lars Maaløe, Søren Kaae Sønderby, and Ole Winther. Ladder variational autoencoders. *Advances in neural information processing systems*, 2016. 2
- [56] Jiaming Song, Chenlin Meng, and Stefano Ermon. Denoising diffusion implicit models. *arXiv preprint arXiv:2010.02502*, 2020. 2
- [57] Yang Song, Conor Durkan, Iain Murray, and Stefano Ermon. Maximum likelihood training of score-based diffusion models. *Advances in neural information processing systems*, 2021. 3
- [58] Stefan Stan, Kazi Injamamul Haque, and Zerrin Yumak. Facediffuser: Speech-driven 3d facial animation synthesis using diffusion. In *Proceedings of the 16th ACM SIGGRAPH Conference on Motion, Interaction and Games*, 2023. 2
- [59] Tiancheng Sun, Jonathan T Barron, Yun-Ta Tsai, Zexiang Xu, Xueming Yu, Graham Fyffe, Christoph Rhemann, Jay Busch, Paul Debevec, and Ravi Ramamoorthi. Single image portrait relighting. *ACM Transactions on Graphics (TOG)*, 2019. 2
- [60] Luan Tran, Xi Yin, and Xiaoming Liu. Disentangled repre-

- sensation learning gan for pose-invariant face recognition. In *Proceedings of the IEEE conference on computer vision and pattern recognition*, 2017. 2
- [61] Arash Vahdat, Karsten Kreis, and Jan Kautz. Score-based generative modeling in latent space. *Advances in neural information processing systems*, 2021. 3
- [62] Ashish Vaswani, Noam Shazeer, Niki Parmar, Jakob Uszkoreit, Llion Jones, Aidan N Gomez, Łukasz Kaiser, and Illia Polosukhin. Attention is all you need. *Advances in neural information processing systems*, 2017. 4, 5
- [63] Eleni Vrochidou, Vladan Papić, Theofanis Kalampokas, and George A Papakostas. Automatic facial palsy detection—from mathematical modeling to deep learning. *Axioms*, 2023. 1
- [64] Zhou Wang, Alan C Bovik, Hamid R Sheikh, and Eero P Simoncelli. Image quality assessment: from error visibility to structural similarity. *IEEE Transactions on Image Processing*, 2004. 6
- [65] Yifan Xia, Charles Nduka, Ruben Yap Kannan, Elena Pescarini, Juan Enrique Berner, and Hui Yu. Afffp: A database with annotated facial landmarks for facial palsy. *IEEE Transactions on Computational Social Systems*, 2022. 1, 6
- [66] Taihong Xiao, Jiapeng Hong, and Jinwen Ma. Elegant: Exchanging latent encodings with gan for transferring multiple face attributes. In *Proceedings of the European conference on computer vision (ECCV)*, 2018. 2
- [67] Sota Yaotome, Masataka Seo, Naoki Matsushiro, and Yen-Wei Chen. Simulation of facial palsy using conditional generative adversarial networks. In *2019 IEEE 8th Global Conference on Consumer Electronics (GCCE)*. IEEE, 2019. 1
- [68] Xi Yin, Xiang Yu, Kihyuk Sohn, Xiaoming Liu, and Manmohan Chandraker. Towards large-pose face frontalization in the wild. In *Proceedings of the IEEE international conference on computer vision*, 2017. 2
- [69] Bohan Zeng, Xuhui Liu, Sicheng Gao, Boyu Liu, Hong Li, Jianzhuang Liu, and Baochang Zhang. Face animation with an attribute-guided diffusion model. In *Proceedings of the IEEE/CVF Conference on Computer Vision and Pattern Recognition*, 2023. 2
- [70] Richard Zhang, Phillip Isola, Alexei A Efros, Eli Shechtman, and Oliver Wang. The unreasonable effectiveness of deep features as a perceptual metric. In *Proceedings of the IEEE Conference on Computer Vision and Pattern Recognition (CVPR)*, 2018. 6
- [71] Wei Zhang, Xianpeng Ji, Keyu Chen, Yu Ding, and Changjie Fan. Learning a facial expression embedding disentangled from identity. In *Proceedings of the IEEE/CVF conference on computer vision and pattern recognition*, 2021. 4
- [72] Hongkai Zheng, Weili Nie, Arash Vahdat, and Anima Anandkumar. Fast training of diffusion models with masked transformers. *arXiv preprint arXiv:2306.09305*, 2023. 3